Investigation of Drug Release and Matrix Degradation of Electrospun Poly(DL-lactide) Fibers with Paracetanol Inoculation

Wenguo Cui, Xiaohong Li,* Xinli Zhu, Guo Yu, Shaobing Zhou, and Jie Weng

School of Materials Science & Engineering, Key Laboratory of Advanced Technologies of Materials, Ministry of Education of China, Southwest Jiaotong University, Chengdu 610031, P.R. China

Received January 19, 2006; Revised Manuscript Received March 13, 2006

This study was aimed at assessing the potential use of electrospun fibers as drug delivery vehicles with focus on the different diameters and drug contents to control drug release and polymer fiber degradation. A drug-loaded solvent-casting polymer film was made with an average thickness of 100 μ m for comparative purposes. DSC analysis indicated that electrospun fibers had a lower $T_{\rm g}$ but higher transition enthalpy than solvent-casting polymer film due to the inner stress and high degree of alignment and orientation of polymer chains caused by the electrospinning process. Inoculation of paracetanol led to a further slight decrease in the T_g and transition enthalpy. An in vitro drug release study showed that a pronounced burst release or steady release phase was initially observed followed by a plateau or gradual release during the rest time. Fibers with a larger diameter exhibited a longer period of nearly zero order release, and higher drug encapsulation led to a more significant burst release after incubation. In vitro degradation showed that the smaller diameter and higher drug entrapment led to more significant changes of morphologies. The electrospun fiber mat showed almost no molecular weight reduction, but mass loss was observed for fibers with small and medium size, which was characterized with surface erosion and inconsistent with the ordinarily polymer degrading form. Further wetting behavior analysis showed that the high water repellent property of electrospun fibers led to much slower water penetration into the fiber mat, which may contribute to the degradation profiles of surface erosion. The specific degradation profile and adjustable drug release behaviors by variation of fiber characteristics made the electrospun nonwoven mat a potential drug delivery system rather than polymer films and particles.

Introduction

Polymers have found increasing applications in the pharmaceutical industry as matrixes for drug delivery systems. Biodegradable polymers provide sustained release of encapsulated drugs and degrade in the body to nontoxic, low-molecularweight products that are easily eliminated. Polymeric drug delivery systems have numerous advantages compared to conventional dosage forms, such as improving therapeutic effects, reducing toxicity, convenience, etc. In addition, a wide variety of polymers, polymer processing techniques, and fabrication techniques are being explored for incorporation of drug molecules into delivery vehicles of various geometries. In particular, sustained release microspheres using biodegradable products such as polylactide (PLA), poly(lactide-co-glycolide) (PLGA), and poly-DL-lactide-poly(ethylene glycol) (PELA) have been investigated.1 This is mainly because of their biocompatibility and the flexibility they offer in terms of their degradation profiles, hydrophilicity, and mechanical properties,² which enable researchers to tailor these polymers to specific applications. Release of pharmaceutical dosage can be designed as rapid, immediate, delayed, pulsed, or modified dissolution depending on the polymer carriers used and other included additives. Microspheres formulations have been extensively investigated, and closed correlations have been quantitatively determined between release profiles and drug distribution in polymer matrix and matrix degradation.³ Other than microspheres, biodegradable polymers have been made into hydrogels,⁴ micelles,⁵ and fibrous scaffolds as drug carriers, each with certain advantages and disadvantages. The main advantage of fibrous carriers is that they offer site-specific delivery of any number of drugs from the scaffold into the body. In addition, the drug can be capsulated directly into fibers with different sizes, and these systems have special properties and surprising results for drug release different from other formulations.

Electrostatic spinning is a versatile polymer processing technique in which a stream of a polymer solution or melt is subjected to a high electric field, resulting in formation of nanodimension fibers. Due to their high specific surface area and porous structure, the electrospun nonwoven fabrics consisting of ultrafine fibers find wide applications as scaffolds for tissue engineering, tissue repair substitutes, wound dressing materials, and carriers for drug delivery.⁶ Drug delivery with polymer nanofibers is based on the principle that the dissolution rate of a drug particulate increases with increased surface area of both the drug and the corresponding carrier if necessary. Furthermore, unlike common encapsulation involving some complicated preparation process, therapeutic compounds can be conveniently incorporated into the carrier polymers using electrospinning. Electrospun nonwoven mats can be cut to almost any size and fabricated into other shapes (e.g., tubes) using different target geometries. The resulting nanofibrous membrane containing drugs can be applied topically for skin and wound healing or postprocessed for other kinds of drug release. Thus, electrospinning show potential as an alternative polymer fabrication technique to drug release systems from particles to fibers.

However, thus far study on drugs encapsulated by polymer nanofibers is still limited. Delivery of a model drug such as tetracycline hydrochloride from nanofibrous membrane, made by electrospinning a blend of poly(ethylene-co-vinyl acetate), poly(lactic acid), and the drug, was reported by Kenawy et al.⁷ It was found that the electrospun nanofibrous mats gave relatively smooth release of drug. For potential use in topical drug administration and wound healing, poorly water-soluble drugs loaded in water-soluble and water-insoluble nanofibrous polymer carriers were investigated.⁸ It was shown that drugloaded polymer nanofibers by electrospinning were able to make the drugs dispersed in an amorphous state, which would facilitate drug dissolution. Rather than simply mixing drugs and carrier polymers before electrospinning, Loscertales et al. developed drug-loaded polymer nanofibers for controlled drug release using coaxial electrospinning,⁹ which aimed to reduce the burst release effect. However, the degradation behavior of drug-loaded superfine fibers and the correlations between drug release and matrix degradation have not yet been investigated. The possibility of controlling drug release through degradation of matrix polymer and fiber characteristics represents an attractive feature for a drug delivery system.

This study was designed to investigate the drug release and matrix degradation profiles of electrospun fibers as a function of fiber characteristics. We focus our attention on the different diameters and drug contents to control drug release and polymer fiber degradation in the drug release system. Poly-DL-lactide with a molecular weight of 78 000 g/mol was used as the matrix polymer and paracetamol, an analgetic drug, was chosen as the model drug. In our previous work the orthogonal experimental method was used to investigate the effect of system parameters on the diameters and morphologies of electrospun fibers. Table $L_{18}(3)^7$ was chosen, and the influencing factors were electric voltage, polymer concentration, molecular weight, solvent, flow velocity, and size of syringe. On the basis of statistical and regression analysis results, optimal processing parameters were applied within the current study. Electrospun fibers with a predetermined diameter and drug loading amount were prepared. DSC analysis was used to determine the thermodynamic profiles of fibers and matrix polymers. In vitro drug release and matrix degradation were investigated and compared with those of polymer films. The water contacting angels of electrospun nonwoven fabrics and solvent-casting films were measured to clarify the different in vitro degradation profiles.

Experimental Sections

Materials. Poly(DL-lactide) (PDLLA) was synthesized in our lab. The molecular weight was determined by gel permeation chromatography (GPC, waters 2695 and 2414, Milford, MA) using polystyrene as a standard. The column used was a Styragel HT 4 (7.8×300 mm). The mobile phase consisted of tetrahydrofuran (THF) using a regularity elution at a flow rate of 1.0 mL/min. Paracetanol was obtained from Kangquan Pharmaceuticals Inc., China. All other chemicals and solvents were of reagent grade or better.

Electrospinning. The electrospinning apparatus was equipped with a high-voltage statitron (Tianjing High Voltage Power Supply Co., Tianjing, China). The polymer and drug were dissolved in a mixture of acetone and chloroform (3/1, v/v) and added in a 5 mL syringe attached to a circular-shaped metal capillary. The circular orifice of the capillary has an inner diameter of 0.6 mm. An oblong counter electrode is located about 15 cm from the capillary tip. The flow rate of the polymer and drug solution was controlled within 3.6–5.4 mL/h by a precision pump (Zhejiang University Medical Instrument Co., Hangzhou, China) to maintain a steady flow from the capillary outlet. The applied voltage was controlled within the range 15–30 kV. Fiber diameters were controlled within 200 nm to 1.5 μ m through optimized processing parameters, and drug loading amounts were kept at 2.0%,

5.0%, and 8.0%. For comparative purposes, cast films were made from PDLLA containing 5.0% paracetanol. The solutions in chloroform were cast onto glass Petri dishes, left at room temperature until the chloroform was evaporated, and then dried under vacuum. All the nonwoven fiber mats and polymer films were vacuum dried at room temperature for 3 days to completely remove any solvent residue prior to the experiments.

Fiber Characterization. The morphology of the electrospunmedicated fibers was investigated by a scanning electron microscope (SEM, Quanta 200) equipped with field-emission gun (10 kV) and Robinson detector after 2 min of gold coating to minimize a charging effect. The fiber diameter was measured from the SEM images, and five images were used for each fiber sample. From each image at least 20 different fibers and 100 different segments were randomly selected and their diameter measured to generate an average fiber diameter using Photoshop 8.0 ed. DSC measurements have been performed using a differential scanning calorimeter (Netzsch STA 449C, Bavaria, Germany). The samples were analyzed in perforated and covered aluminum pans under a nitrogen purge. Approximately 1 mg of polymer or fiber sample was heated from 25 to 150 °C with a heating rate of 10 °C/ min. To clarify different in vitro degradation profiles between electrospun nonwoven fabrics and solvent-casting films, the contact angles of water and poly(ethylene glycol) water solution on the surface were measured in the current study. Contact angles were measured with a JY-82 contact angle goniometer (Chengde, China). The final result was obtained by averaging at least five separate runs, and the surface tension was calculated accordingly.¹⁰

In Vitro Drug Release Behaviors of Electrospun Nonwoven Fabrics. The electrospun nonwoven fabrics and solvent-casting polymer film with drug entrapment were first sectioned into $2 \times 2 \text{ cm}^2$ squares, and the drug content was determined as a function of scaffold weight. Each square sample was incubated into 20.0 mL of 154 mM phosphatebuffered saline (PBS), pH 7.4 \pm 0.1, containing 0.02% sodium azide as a bacteriostatic agent. The suspension was kept in a thermostated shaking water bath (Taichang Medical Apparatus Co., Jiangsu, China) that was maintained at 37 °C and 100 cycles/min. Samples of 1.0 mL released solution were taken from the dissolution medium at 4, 8, 12, 24, 48, 96, 144, 240, and 336 h after incubation, while an equal amount of fresh PBS was added back to the incubation solution. The amount of paracetanol was detected with a UV-vis spectrophotometer (UV-2550, Shimadzu, Japan), and a maximal absorption peak of 243 nm was observed for freshly prepared paracetanol in PBS and released within the designed period. For standard samples with a concentration from 0 to 20 μ g/mL, a linear correlation ($\gamma^2 = 0.9999$) was determined between the absorption strength and paracetanol concentration. The percentage of the released drug in triplicate samples was then calculated based on the initial weight of the drug incorporated in the electrospun scaffold. The structure integrity of released paracetanol was determined by high-performance liquid chromatography (HPLC) with a UV detector set at 243 nm (Waters 2695 and 2487, Milford, MA) using fresh paracetanol as a standard. C18 stationary phase with a 5 μ m particle size and column dimensions of 4.6 \times 150 mm i.d. was used, and the mobile phase consisted of 0.1 M phosphate buffer (pH 4.5) and methanol (80/20 vol %) at a flow rate of 1.0 mL/min.

In Vitro Matrix Degradation Behaviors of Electrospun Nonwoven Fabrics. The degree of degradation was estimated from the change in morphology, the decrease in molecular weight, and the mass loss. Preweighted pieces of electrospun nonwoven fabrics and solventcasting polymer film (about 150 mg each) were incubated in 20.0 mL of PBS as described above. At predetermined intervals triplicate samples for each kind of fabric or film were recovered, rinsed with distilled water to remove residual buffer salts, and dried to constant weight in a vacuum desiccator. The mass loss was determined gravimetrically by comparing the dry weight remaining at a specific time with the initial weight. The recovered and dried fabrics or films were dissolved in THF and filtered to eliminate insoluble residues. The molecular weight of recovered matrix polymer was determined using GPC as described above.

Table 1. Process Parameters and Characteristics of Electrospun Fibers under Investigation

	flow					
	drug	polymer	voltage	velocity		
sample	added (%)	concentration (%)	(kV)	(mL/h)	diameter (nm)	SD (nm)
а	5.0	18.0	20	3.6	211.6	56.2
b	5.0	23.0	20	5.4	550.9	46.4
С	5.0	30.0	20	5.4	1309.5	110.4
d	2.0	23.0	25	5.4	371.1	63.5
е	5.0	23.0	20	3.6	408.2	47.7
f	8.0	23.0	20	5.4	388.6	59.2

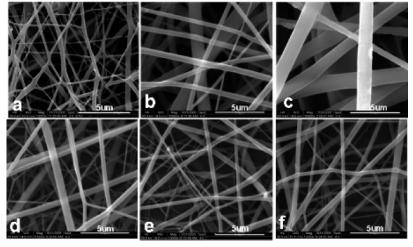


Figure 1. SEM photographs of electrospun PDLA fibers with paracetanol inoculation. a-f refer to sample a-f in Table 1.

Results and Discussion

Electrospinning is a simple process for the production of fibers with diameters in the submicrometer to micrometer range. The simplest setup consists of only a syringe or pipet to hold the polymer solution, two electrodes, and a DC high-voltage power generator. In addition, electrospinning seems to be the only method which can be further developed for large-scale production of continuous nanofibers for industrial applications. A broad range of applications for electrospun fibers have been suggested including drug delivery, which has been demonstrated from biodegradable polymeric fibers for antibiotics,¹¹ and DNA for gene therapy.¹² The small fiber diameters produced by electrospinning have the advantage of a large surface-to-volume ratio as well as a high permeability and interconnecting pore structure, both of which are desirable to control the drug loading and release profiles.

Fiber Characterization. In the current study the drug release and matrix degradation profiles of the electrospun mat were investigated with respect to different fiber diameters and drug loading amounts. Electrospun fibers with a drug loading amount of 5.0% and diameters of 212 nm, 551 nm, and 1.31 µm were prepared. Also, fibers with sizes of around 400 nm but with a different drug entrapment of 2.0%, 5.0%, and 8.0% were prepared. In a previous study the orthogonal experimental method was used to investigate the effect of system parameters on the diameters and morphologies of electrospun fibers (data not shown). Among the influencing factors such as electric voltage, polymer concentration, molecular weight, solvent, flow velocity, and size of syringe, a significant influence was observed for polymer molecular weight and solution concentration on fiber diameters (p < 0.05), and there were also significant effects due to polymer molecular weight, solution concentration, solvent system, nozzle size, and applied voltage on fiber morphologies (p < 0.05). Regression analysis revealed

quantitative relations between fiber properties (diameters and spindle percent) and electrospinning parameters (polymer molecular weight and solution concentration). These results were essential to obtain the optimized parameters in the current study to prepare a fibrous mat with a predetermined size and morphology.

Table 1 summarizes the process parameters for each kind of sample and the characteristics of the resulting fibers. All the electrospun-medicated mats are opaque due to light scattering by the fine fibers. Figure 1 shows uniform fibers without any beads for all samples with different diameters and amounts of drug entrapment. The thickness was typically controlled between 200 and 250 μ m. In the experiment it was found that addition of a small molecule drug led to formation of uniform but smaller fibers. The possible reason for this improvement is that addition of drugs disturbed the polymer solution, lowered the surface tension, and thus enhanced the bending instability.¹³ In the UVvis measurements the spectra of pure and released paracetanol (from two separate scaffolds and at three time points) showed a similar maximum absorbance peak at 243 nm. HPLC analysis showed the same elution time of 4.73 min for pure and released paracetanol. Thus, it can be concluded that the chemical structure of the released paracetanol appears to be intact after electrospinning processing.

DSC Analysis of Electrospun Nonwoven Fiber Mat. To date few reports have focused on the effect of the electrospinning process on the thermodynamic behavior of the obtained fibers. To determine the effect of electrospinning and drug inoculation on the thermodynamic behavior, DSC traces of electrospun mat with and without drug entrapment and solvent-casting polymer film were recorded, and they are shown in Figure 2. A lower glass transition temperature (T_g) was observed for electrospun nonwoven mat (54.6 °C) than polymer films (61.7 °C). These results were ascribed to the inner stress and the high degree of

DSC/(mW/mg)

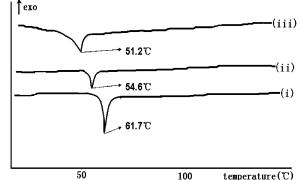


Figure 2. DSC traces of solvent-casting polymer film (i) and electrospun nonwoven fiber mat without (ii) and with (iii) drug entrapment.

alignment and orientation of polymer chains caused by the electrospinning process. With increasing temperature, movement of the polymer chains driven by the inner stress occurred at a lower $T_{\rm g}$. To clarify the driven force of inner stress, DSC analysis of electrospun mats with diameters of 212 nm (sample a), 551 nm (sample b), and 1.31 μ m (sample c) was performed and T_{gs} of 49.8, 51.2, and 53.5 °C were observed, respectively. The smaller the diameter of the fiber, the more energy could be restocked to lead to the decreasing glass state temperature. Figure 2 also shows that the paracetanol inoculation into the fiber mat led to a lower T_g (51.2 °C). By adding drug into the electrospinning polymer fibers, the small molecule drug acted on the molecular chains and made the molecular chains move easily, leading to a lower $T_{\rm g}$. In addition, the higher drug content in the polymer fiber led to the better chain extenders to make molecular chains smoother. Samples with a small diameter but with 2% (sample d), 5% (sample e), and 8% (sample f) of drug entrapment showed T_g at 51.2, 50.3, and 47.3 °C, respectively.

The glass transition enthalpy was 7.55, 12.75, and 2.84 J/g for the electrospun mat with and without drug entrapment and the solvent-casting polymer film, respectively. The inner stress of the polymer chain of electrospun fibers resulted in a significantly higher transition enthalpy than that of polymer films. In addition, drug inoculation led to irregular alignment of the polymer chain, which led to a slight decrease in the transition enthalpy.

In Vitro Paracetanol Release from Electrospun Fiber Mat. Electrospun fibers with the same drug entrapment of 5.0% but with diameters from 200 nm to 1.31 μ m and fibers with sizes of around 400 nm but with different drug entrapments of 2.0%, 5.0%, and 8.0% were investigated for drug release profiles. To compare the different degradation and drug release profiles, drug-loaded solvent-casting polymer film was made with an average thickness of 100 μ m. Figures 3 and 4 show the paracetanol release profiles from the electrospun mat and polymer films. The release profiles of all systems were characterized by a typical biphasic pattern. In the initial phase a pronounced burst release or steady release phase was observed, and then it tended to a plateau or a gradual release followed during the rest time.

Figure 3 shows the profiles of paracetanol release from polymer film, electrospun fibers with 5.0% of drug entrapment and with a size of 212 nm, 551 nm, and 1.31 μ m. All electrospun fibers exhibited a linear release behavior during the first stage. Nearly zero-order release profiles were observed during the first 24, 48, and 96 h, and the total amount of release was 80%, 50%, and 80% during this stage and detected for fibers with a

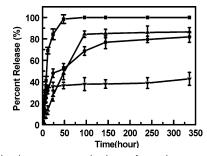


Figure 3. In vitro paracetanol release from electrospun fibers with 5.0% of drug entrapment and fiber diameters of 212 (\blacksquare), 551 (\bullet), and 1.31 μ m (\blacktriangle) and casting polymer film with a thickness of 100 μ m (\bigtriangledown).

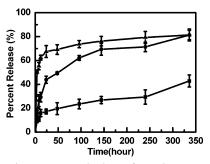


Figure 4. In vitro paracetanol release from electrospun fibers with 2.0% of drug entrapment and size of 389 nm (\blacksquare), 5.0% of drug entrapment and size of 408 nm (\bullet), and 8.0% of drug entrapment and size of 371 nm (\blacktriangle).

size of 212 nm, 551 nm, and 1.31 μ m, respectively. On the basis of our previous study,¹⁴ the initial inner structure and the dispersion pattern of drug within the polymer matrix should be considered as critical factors controlling the release process. It would likely be deduced from the linear release behavior of the electrospun fiber mat that drug molecules dispersed throughout the mat matrix. The porous structure of the fiber mat and the pores after diffusion out of drug molecules from the outer layer made it possible to further constant release of the drug from the inner part.

However, for solvent-casting polymer films a large initial burst at short times and minimum sustained release at longer times were observed. Twenty-five percent of burst release was observed during the initial 4 h followed by nearly no more release in the next 2 weeks. This behavior is different from that in the medicated electrospun fiber with the same drug content. The paracetanol molecules dispersing close to the polymer film surface were those adsorbed at or loosely bound near the surface, which diffused in the initial incubation time. Also, only around 40% of the included drug has been detected for polymer films in the release medium within 2 weeks; the other 60% was still entrapped into the film, which maybe would not release out until significant degradation of the matrix polymer occurred.

Figure 4 summarizes the paracetanol release profile from fibers of around 400 nm but with drug entrapments of 2.0%, 5.0%, and 8.0%. When the amount of drug entrapment was increased, the drug molecules may aggregate more on the fiber surface, which would lead to an even larger initial burst of drug. There was about 50% of release in the initial 4 h as seen in the fiber mat with 8.0% of drug entrapment. When the concentration of drug decreases to 5% fibers, it will have better sustain release compared to 8%. However, for drug entrapment of 2.0%, a slow and continuous release happened in the first 16 h but minimum further release was detected up to 2 weeks. During the electrospinning process paracetanol would disperse throughout

Investigation of Drug Release and Matrix Degradation

the fiber mat and a large amount would distribute at or close to the fiber surface when drug entrapment increased. However, most of the drug was entrapped within the fibers of lower drug inoculation. For fibers with 2.0% of drug entrapment, the lower porosity of fibers created by initial diffusion of drug, due to lower drug entrapment, would lead to slow release in the following stages. The pores left after drug diffusion were critical for further release from the inner sections of fibers through the swollen and porous inner structure because liquid is difficult to enter into inside of the nonwoven fibers which have been thickly dotted with layer upon layer fibers.

Thus, from these data it may be concluded that the drug release profiles from electrospun-medicated fibers can be adjusted through fiber size and drug inoculation amount. Delayed release behaviors obtained from the above investigation demonstrated potential for programmed delivery by variation of the fiber characteristics for clinical needs. Fibers with different diameters exhibited a different length of period of nearly zeroorder release, and higher drug encapsulation led to more significant burst release after incubation. Dependent on the pathological conditions and drug properties, pharmaceutical kinetics would be optimized using the electrospun fiber formulations with combined fiber size and drug loading amount. For example, fibers with larger drug entrapment were more suitable for delivery of antibiotic drugs to potentially prevent surgeryinduced infections. The larger initial burst was actually ideal since it was important to eliminate intruding bacteria before they began to proliferate. However, for those that may survive the initial burst, a continued release of antibiotic was also necessary to prevent further population.

In Vitro Degradation of Electrospun Fiber Mat. To date more attention has been paid to drug release than matrix degradation for electrospun fibers. For biomedical applications, especially for drug delivery systems, a suitable degradation rate was the most important requirement for matrix materials. Electrospun fibers possess a specific surface area between films and nano- or microparticles, and therefore, moderate biodegradation rates were expected. Zone et al.¹⁵ reported the in vitro degradation behavior of electrospun poly(glycolide-co-lactide) ultrafine fibers, which exhibited a sudden increase in crystallinity and glass transition temperature due to the fast thermally induced crystallization process. The continuous increase in crystallinity and apparent crystal size as well as the decrease in long period and lamellae thickness indicated that the thermally induced crystallization was followed by a chain cleavage. Zeng et al.¹⁶ investigated the degradation of poly(L-lactide) and $poly(\epsilon$ caprolactone) electrospun fibers under catalysis of proteinase K. The PLLA fibers containing the anionic surfactant sodium docecyl sulfate (SDS) exhibited a faster degradation rate than those containing cationic surfactant triethylbenzylammonium chloride (TEBAC), indicating that surface electric charge on the fibers is a critical factor for enzymatic degradation. In the current study the degradation profiles of fibers with different sizes and drug encapsulation were investigated with respect to changes in morphology, fiber mass, and molecular weight of matrix polymer.

After incubation into the degradation medium, the nonwoven fibrous mat floated on the PBS first and then suspended and immersed into the medium. Meanwhile, nonwoven mat changed from shrinking to puffing bigger than before. Figure 5 shows the morphologies of degraded medicated fibers with different sizes and drug inoculations after 4 and 9 weeks. It is indicated that fiber size increased and fiber space decreased for all samples, while different morphologies appeared with fibers of

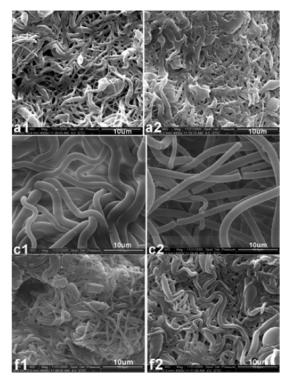


Figure 5. SEM morphologies of electrospun fibers with 5.0% of drug entrapment and size of 212 nm (a), 5.0% of drug entrapment and size of 1.31 μ m (c), and 8.0% of drug entrapment and size of 389 nm (f) after being incubated 4 (a1,c1, and f1) and 9 weeks (a2, c2, and f2) (×4000).

different characteristics after incubation into the degradation medium. As shown in the SEM photos at week 4, all the fibers were swollen compared with the original formation shown in Figure 1 due to chain relaxation of the matrix polymer after incubation into the medium with elevated temperature. In addition, the lower T_g of fiber mat led to more significant changes in fiber morphologies. Fibers with a large diameter (c1) exhibited less variation in fiber morphology than smaller fibers (a1) with lower T_{g} . Also, the fibers with higher drug inoculation (f1) exhibited the same phenomenon as thinner fibers (a1) due to the close glass transition temperatures. At week 9 after incubation, bundles of the thinner fibers (a2) and fibers containing more drug (f2) had almost solidified into larger melted structures as a consequence of the fiber swelling and drug releasing. In other words, the smaller diameters and higher drug entrapment led to more significant changes of morphology after fibers were incubated into the degradation medium.

Gravimetric evaluation of the loss of electrospun fiber mat and polymer films during incubation is summarized in Figure 6A. The mass loss of the fibers and film in the early stage may result from a lower molecular part of the polymers and small molecule drug on the fiber surface dissolving into the degradation medium. In the middle stage of degradation, the slight weight loss may be caused by the drug diffusing out and polymer degrading. Note that no mass loss occurred in polymer films and electrospun fibers with 1.31 μ m over the incubation period, excluding around 5% of drug release out from the polymer matrix. There were total 10% and 20% mass loss for electrospun fibers with a diameter of 212 and 551 nm, respectively. Figure 6B shows the molecular weight loss of polymer matrix of fiber mat and polymer films. Almost no molecular weight reduction was found for electrospun fiber mat, but the molecular weight of polymer films decreased gradually with incubation time and around 50% loss was detected after 9

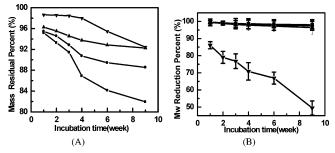


Figure 6. Residual mass percent (A) and molecular weight reduction (B) of electrospun fiber mats with 5.0% of drug entrapment and fiber diameters of 212 nm (\blacksquare), 551 nm (\bullet), and 1.31 μ m (\blacktriangle) and casting polymer film with a thickness of 100 μ m (\checkmark) after incubating in PBS at 37 °C.

 Table 2.
 Wetting Behaviors of Electrospun Fibers and Polymer

 Films
 Films

samples	water contact angle (deg)	surface tension (mN/m)
electrospun fiber ^a polymer film	$ \begin{array}{r} 140.1 \pm 7.8 \\ 69.5 \pm 6.6 \end{array} $	1.51 33.8

^a Fibers with size of 551 nm and drug inoculation of 5.0%.

weeks incubation. This was somewhat unexpected for electrospun fibers due to the porous structure and high specific surface area of electrospun fibers, which should result in faster matrix breakdown compared with the solid polymer films.

For solvent-casting polymer film no apparent mass loss but a significant decrease in molecular weight was detected during the incubation period. The mass loss began when a fraction of the degradation products soluble in degradation medium were generated from the polymers. The onset for mass loss lagged behind molecular weight reduction; thus, hydrolysis of polymer films should proceed through the bulk of the polymer structure, which was in good agreement with the bulk degradation mechanism of polylactide. However, electrospun fiber mats showed different degradation behaviors, that is, almost no molecular weight reduction was detected but mass loss was observed for fibers with small and medium size. Obviously this was not consistent with the bulk degradation mechanism of common formulations of PLA and seemed more likely to be the surface erosion mechanism. As we know, the difference between the breakdown velocity of a chemical bond of matrix polymer and the distribution speed of water into the polymer matrix would determine the degradation mechanism for most of the biodegradable polymers. Degradation based on the surface erosion mechanism would occur when water penetration is slower than matrix breakdown. It was suggested that the slower water distribution speed from the medium to the fiber matrix be due to changes in the wetting behavior after the electrospinning process in the current system.

Wetting Behaviors of Electrospun Fiber Mat. Recently, Stephens et al. found that electrospinning greatly affected the secondary structure of the silk analogue, yielding protein backbones that exhibit predominantly an α -helical rather than the original β -sheet conformation.¹⁷ To clarify the effect of the electrospinning process on the surface properties of electrospun fibers, water contact angles of electrospun fibers and polymer films were measured and the surface tension calculated, which is summarized in Table 2. A more hydrophobic surface was observed for electrospun fiber mat than that of polymer films. The high water repellent property of electrospun fiber led to much slower water penetration into the fiber mat, which may contribute to the degradation profiles of surface erosion.

The remarkable hydrophobic properties of electrospun fiber mat have attracted much attention to uncover the reasons. Acatay et al. fabricated electrospun films with a high degree of roughness consisting of fibers and clustered beads and found that the high hydrophobicity of the entire electrospun membrane resulted from its nanofibrous topography.¹⁸ As we know, the electrospinning process involved use of a polymer solution that was contained in a syringe and held at the end of the needle by its surface tension. Charge was induced on the solution by an external electric field. As the applied electric field was increased, charges created directly opposed the surface tension. Bevond a critical value the electric field caused the charges to overcome the surface tension and form a charged jet of solution. During the electrospinning process the high surface tension at the air/ polymer interface, the aligning effect of the elongational flow, and rapid solidification are believed to have some effects on the surface wetting properties. Air bubbles entrapped within the irregular surface and between fibers and/or enrichment of chemical elements or groups due to the high voltage of the electrospinning process should have a large effect on the hydrophobicity of electrospun fibers and fiber mats. Further investigations on the surface morphology, the microphaseseparated structures, and the effect of electrospinning parameters are ongoing to test these hypotheses.

Conclusions

DSC analysis indicated that electrospun fibers had a lower T_{g} but higher transition enthalpy than solvent-casting polymer film. An in vitro drug release study showed that a pronounced burst release or steady release phase was initially observed followed by a plateau or gradual release during the rest time. Electrospun fiber mat showed almost no molecular weight reduction, but mass loss was observed for fibers with small and medium size, which was characterized by surface erosion and inconsistent with the ordinarily polymer degrading form. Further wetting behavior analysis showed that the high water repellent property of the electrospun fiber led to much slower water penetration into the fiber mat, which was attributed to the degradation profiles of surface erosion. Therefore, electrospun fibers with specific degradation profiles and adjustable drug release profiles by variation of fiber characteristics has potential use as new drug carriers instead of films and particles.

Acknowledgment. This work was partially supported by the National Natural Science Foundation of China (30570501), Specialized Research Fund for the Doctoral Program of Higher Education (20050613025), Fok Ying Tung Education Foundation (104032), and Cultivation Fund of the Key Scientific and Technical Innovation Project, Ministry of Education of China.

References and Notes

- Kissel, T.; Li, Y. X.; Volland, C.; Gorich, S.; Koneberg, R. J. Controlled Release 1996, 39, 315.
- (2) Zhou, S. B.; Liao, X. Y.; Li, X. H.; Deng, X. M.; Li, H. M. J. Controlled Release 2003, 86, 195.
- (3) Li, X. H.; Deng, X. M.; Huang, Z. T. Pharm. Res. 2001, 18, 117.
- (4) Mason, M. N.; Metters, A. T.; Bowman, C. N.; Anseth, K. S. *Macromolecules* 2001, 34, 4630.
- (5) Hagan, S. A.; Coombes, A. G. A.; Garnett, M. C.; Dunn, S. E.; Davies, M. C.; Illum, L.; Davis, S. S.; Harding, S. E.; Purkiss, S.; Gellert, P. R. *Langmuir* **1996**, *12*, 2153.
- (6) Zhang, Y. Z.; Lim, C. T.; Ramakrishna, S.; Huang, Z. M. J. Mater. Sci. Mater. Med. 2005, 16, 933.
- (7) Kenawy, E. R.; Bowlin, G. L.; Mansfield, K.; Layman, J.; Simpson, D. G.; Sanders, E. H.; Wnek, G. E. J. Controlled Release 2002, 81, 57.

Investigation of Drug Release and Matrix Degradation

- (8) Verreck, G.; Chun, I.; Rosenblatt, J.; Peeters, J.; Dijck, A. V.; Mensch, J.; Noppe, M.; Brewster, M. E. J. Controlled Release 2003, 92, 349.
- (9) Loscertales, I. G.; Barrero, A.; Guerrero, I.; Cortijo, R.; Marquez, M.; Gana-Calvo, A. M. Science 2002, 295, 1695.
- (10) Lau, K. K. S.; Bico, J.; Teo, K. B. K.; Chhowalla, M.; Amaratunga, G. A. J.; Milne, W. I.; McKinley, G. H.; Gleason, K. K. *Nano Lett.* 2003, *3*, 1701.
- (11) Kim, K.; Luu, Y. K.; Chang, C.; Fang, D. F.; Hsiao, B. S.; Chu, B. J. Controlled Release 2004, 98, 47.
- (12) Luu, Y. K.; Kim, K.; Hsiao, B. S.; Chu, B.; Hadjiargyrou, M. J. Controlled Release 2003, 89, 341.
- (13) Zeng, J.; Xu X. Y.; Chen, X. S.; Liang, Q, Z.; Bian, X, C.; Yang, L, X.; Jing X. B. J. Controlled Release 2003, 92, 227.

- (14) Li, X. H.; Deng, X. M.; Yuan, M. L.; Xiong, C. D.; Huang, Z. T.; Zhang, Y. H.; Jia, W. X. J. Appl. Polym. Sci. 2000, 78, 140.
- (15) Zong, X. H.; Ran, S. F.; Kim, K. S.; Fang, D. F.; Hsiao, B. S.; Chu, B. Biomacromolecules 2003, 4, 416.
- (16) Zeng, J.; Chen, X. S.; Liang, Q. Z.; Xu, X. L.; Jing, X. B. Macromol. Biosci. 2004, 4, 1118.
- (17) Stephens, J. S.; Fahnestock, S. R.; Farmer, R. S.; Kiick, K. L.; Chase, D. B.; Rabolt, J. F. *Biomacromolecules* **2005**, *6*, 1405.
- (18) Acatay, K.; Simsek E.; Ow-Yang C.; Menceloglu Y. Z. Angew. Chem., Int. Ed. 2004, 43, 5210.

BM060057Z